

Indole-3-carbinol induces apoptosis in human hepatocellular carcinoma Huh-7 cells



Chang Min Lee^a, Yong Jun Choi^a, See-Hyoun Park^{b,*}, Myeong Jin Nam^{a,*}

^a Department of Biological Science, Gachon University, Seongnam, Republic of Korea

^b Department of Bio and Chemical Engineering, Hongik University, Sejong 30016, Republic of Korea

1. Introduction

In some regions of Asia and Africa, liver cancer is the most common cancer, where it accounts for 15% of all deaths (Kim et al., 2010). Although many treatments for liver cancer have been developed, these therapies have several drawbacks, such as the detrimental effects of radiation therapy on normal liver tissue (Demaria et al., 2015; Lasley et al., 2015). Therefore, there is significant interest in developing novel therapeutic agents for the treatment of liver cancer with fewer side effects.

Plants produce various phytochemicals, which are chemical substances produced by plants that help them thrive and act against pathogens, predators, or competitors. Phytochemicals can be divided into several categories, including flavonoids and polyphenols. I3C is a typical phytochemical found naturally in cruciferous vegetables such as kale, sprouts, and cabbage (Sherer et al., 2017). I3C is known to suppress the proliferation of many type of cancer, such as human breast, colon, prostate and endometrial cancer (Bai et al., 2013), and there are many studies demonstrating the anti-cancer effects of I3C in many types of cancer cells. Moreover, I3C can act as an anti-oxidant in osteoblasts by suppressing cytotoxicity and can induce apoptosis in osteoblastic cells (Lin et al., 2015). I3C also has significant suppressive effects of prostate cancer cells both in vitro and in vivo (Souli et al., 2008). In addition, I3C induces apoptosis in the human lung epithelial carcinoma A549 cells by regulating p53 and the caspase-8 pathway (Choi et al., 2010). However, the anti-cancer effects of I3C in human liver cancer have not been investigated.

Protein expression profiling has aided in determining the proteins expressed in various cancers. This technique provides important information on specific cancer biomarkers (Srinivas et al., 2002). In this study, we performed 2-DE to compare the differentially expressed proteins between untreated control and 500 μM I3C-treated Huh-7 cells. We found that the expression level of heat shock protein 27 (Hsp27) was increased in I3C-treated Huh-7 cells compared to the expression in untreated control cells. We confirmed this result by western blotting using an Hsp27-specific antibody.

Heat shock proteins (Hsps) have many functions, including protein

activity modulating, protein degradation controlling, and protein translocation inducing activities (Concannon et al., 2003a). One important function of heat shock proteins is the regulation of apoptosis (Concannon et al., 2003a), and Hsp27 has been shown to inhibit apoptosis signaling in various ways. However, there are only a few studies demonstrating Hsp27-mediated induction of apoptosis in cancer cells. For example, overexpression of Hsp27 in pancreatic cancer cells induces cell cycle arrest and apoptosis (Guo et al., 2015).

The objective of our study was to investigate the anti-cancer effects of I3C in Huh-7 human hepatocellular carcinoma cells and describe the functions of I3C in modulating Hsp27 expression and activation of apoptotic pathways.

2. Materials and methods

2.1. Reagent

I3C was purchased from Sigma-Aldrich (St. Louis, MO, USA) and dissolved in dimethyl sulfoxide (DMSO). A 0.4 M stock solutions of I3C was stored at –20 °C.

2.2. Cell culture

Huh-7 cells and WRL68 cells were purchased from the Korean Cell Line Bank (Seoul, Korea) and were maintained under standard conditions (5% CO₂, 37 °C and 95% humidity). The cells were cultured in Dulbecco's modified Eagle's medium (DMEM; GIBCO, Grand Island, NY, USA) containing 1% penicillin/streptomycin (GIBCO) and 10% heat-inactivated fetal bovine serum (GIBCO). For the experiments, the cells were harvested at 80% confluence using 0.25% (w/v) trypsin-EDTA (Sigma-Aldrich, St. Louis, MO, USA), and 24 h after seeding, the medium was exchanged for new medium containing I3C (Sigma-Aldrich, St. Louis, MO, USA) dissolved in dimethyl sulfoxide (DMSO). Control cells were cultured in medium containing the same amount of DMSO.

* Corresponding author.

** Corresponding author. Department of Bio and Chemical Engineering, Hongik University, Sejong-si, Republic of Korea.

E-mail addresses: shpark74@hongik.ac.kr (S.-H. Park), genetx@hanmail.net, genetxnam@gmail.com (M.J. Nam).

2.3. Cell viability assay, MTT and WST-1

Cells were seeded in 96-well plates at a density of 3×10^3 cells per well and incubated for 24 h. Then, the cells were washed with phosphate buffered saline (PBS), and medium containing different concentrations of I3C (0, 300, 500, and 700 μM) was added. After 24 h of treatment, 20 μL of 3-(4, 5-dimethylthiazol-2yl)-2, 5-diphenyl-2H-tetrazolium bromide (MTT) solution (1 mg/mL) was added to each well, and the cells were incubated for 2 h under standard conditions (5% CO₂, 37 °C, 95% humidity). After incubation, the medium was removed, and 200 μL of DMSO was added to each well. The plate was placed on a shaker for 30 min, and then the level of formazan was measured using a spectrophotometer at 570 nm. In WST-1 assay, After 24 h of I3C treatment, 10 μL of EZ-Cytotoxicity (dozen Bio, Korea) was added to each well and the cells were incubated for 1 h under standard conditions (5% CO₂, 37 °C, 95% humidity). After incubation, the level of formazan was measured using a spectrophotometer at 450 nm.

2.4. Colony formation assay

Huh-7 cells (100 in each well) were seeded in 6-well plates and incubated for 24 h under standard conditions (5% CO₂, 37 °C, 95% humidity). After 24 h, the medium was exchanged for fresh medium containing I3C or DMSO (control). After 24 h, the medium was replaced again. Three days later, the cells were washed with PBS twice for 5 min each. Then, the cells were treated with 1 mL of 4% formaldehyde for 20 min, and washed twice with PBS, as described above. Then, 1% crystal violet was added, and the cells were incubated at room temperature for 30 min. Then, the cells were washed with distilled water, and imaged for analysis.

2.5. Western blotting

Huh-7 cells (8×10^6) were harvested and lysed in lysis buffer containing RIPA buffer, protease inhibitor (Sigma-Aldrich, St. Louis, MO, USA), and phenylmethylsulfonyl fluoride (Sigma-Aldrich, St. Louis, MO, USA). The protein concentration of the cell lysate was measured using a Qubit™ Fluorocytometer (Invitrogen). Proteins were separated by SDS-PAGE (sodium dodecyl sulfate polyacrylamide gel electrophoresis) at 120 V for 2 h and electrophoretically transferred to a nitrocellulose membrane at 55 V for 2 h. The membranes were blocked with albumin (Biosesang, Korea), and then incubated with primary antibodies against various apoptosis-related proteins (β-actin, PARP, cleaved-PARP, caspase-3, -7, -9, cleaved caspase-3, -7, -9, p53, Hsp27, Cell Signaling Technology) at 4 °C overnight. Then, the membranes were washed with TBS-T, and fluorescence was measured using the Chemi-doc detection system (Bio-Rad, USA). Primary antibodies were purchased from Cell Signaling Technology and Santa Cruz. We recorded catalog number and lot number. Cell Signaling Technology: (Actin: #4970, 14), (Akt: #9272, 27), (pAkt: #4056, 11), (ERK: #4696, 3), (pERK: #4370, 7), (JNK: #9252, 9), (p38: #9212, 13), (bad: #9292), (pbad: #5284, 3), (P53: #9282, 4), (PARP: #9542, 10), (cleaved PARP: #9541, 6), (caspase-3: #9662, 12), (cleaved caspase-3: #9664, 18), (caspase-7: #9492, 6), (cleaved caspase-7: #9491, 7), (caspase-9: #9502, 8), (cleaved caspase-9: #7239). Santa Cruz: (MDM2: sc-965, J2413). Secondary antibodies were purchased from Cell Signaling Technology (Rabbit, #7074, 27) and Santa Cruz (Mouse, sc-2005, D0116).

2.6. 2-Dimensional gel electrophoresis

Huh-7 cells (7×10^6 cells) were treated with 500 μM I3C for 24 h. Then, these cells were harvested and lysed in lysis buffer (7 M urea, 2 M thiourea, 2% CHAPS, 20 nM DTT, 0.5% pharmalyte, and protease inhibitor). Lysed protein samples were loaded onto a dryStrip (18 cm, pH 3–10; GE Healthcare, Little Chalfont, UK). For the first dimension

separation, IEF was performed in a Multiphor II IEF system (GE Healthcare) at 24 °C. After IEF, the IPG strips were incubated in equilibration buffer (75 nM Tris-HCl, pH 8.8, containing 6 M urea, 29.3% glycerol, 2% SDS (sodium dodecyl sulfate), and 0.02% bromophenol blue) for 10 min, twice. Then, the proteins were applied to 12.5% SDSpolyacrylamide gels using an Ettan DALTsix vertical electrophoresis system (GE Healthcare). The proteins in the gels were visualized by Coomassie blue staining, and the spot patterns of the control and I3C-treated cells were compared. Relevant protein spots were extracted from the 2-DE gels and identified by MALDI-TOF.

2.7. Annexin V/PI staining

The FITC Annexin V apoptosis detection kit (BD Bio-Sciences, Franklin Lakes, NJ, USA) was used to detect I3C-induced apoptosis. Huh-7 cells were seeded in a 6-well plate at a density of 3×10^5 cells per well. After 24 h, the cells were treated with different concentrations of I3C (0, 100, and 300 μM). After 24 h of treatment, the cells were washed with PBS and resuspended in binding buffer, followed by labeling with FITC Annexin V for 15 min at room temperature in the dark. Then, the cells were analyzed by flow cytometry.

2.8. Terminal deoxynucleotidyl transferase (TdT)-mediated dUTP nick-end labeling assay

We performed TUNEL assay using the fluorometric TUNEL system (Promega, Madison, WI, USA) to detect the fluorescence in apoptotic cells. Huh-7 cells were seeded in 6-well plates at a density of 1.5×10^5 per well and incubated for 24 h. The cells were fixed with 4% formaldehyde for 25 min, permeabilized using 0.5% Triton X-100 for 5 min. The cells were treated with 50 μL TdT enzyme buffer (Equilibration buffer 45 μL , Nucleotide mix 5 μL , TdT enzyme 1 μL). Cell nucleus was dyed by Hoechst Stain Solution (Sigma-Aldrich, St. Louis, MO, USA). 5 μL Hoechst Stain Solution was dissolved in 10 mL PBS and each well was treated 2 mL respectively. DNA fragmentations were detected by fluorescence microscope (Nikon Eclipse TE 2000-U, Tokyo, Japan).

2.9. Transfection

Huh-7 cells were seeded at a density of 2×10^5 cells in a six-well culture dish. After 24 h, transfection with 30 nM Hsp27-siRNA (Cell Signaling Technology) or control-siRNA (Santa-Cruz) was performed with Lipofectamine 2000 (Invitrogen) and Opti-Mem (GIBCO). Cells plated at 60% confluence in 6-well plates were transfected at 4 h. After 4 h, media was changed into completed media (containing 10% FBS, 1% antibiotics).

2.10. Statistical analysis

The values shown are representative data from three or more independent experiments. One way ANOVA followed by Bonferroni's post hoc test was used for statistical analysis, and a p value less than 0.05 was considered statistically significant.

3. Results

3.1. I3C inhibited proliferation of Huh-7 cells

To investigate the anti-proliferation effects of I3C in liver cancer, we first examined the impact of I3C on the viability of the human hepatocellular carcinoma cell line Huh-7 cells. For this experiment, Huh-7 cells were treated with 0, 300, 500, and 700 μM I3C dissolved in DMSO (final concentration, 0.125%) for 24 h and 48 h, and then analyzed by the MTT assay. As shown in Fig. 1A, I3C has a dose- and time-dependent anti-proliferative effect in Huh-7 cells. Cell proliferation was

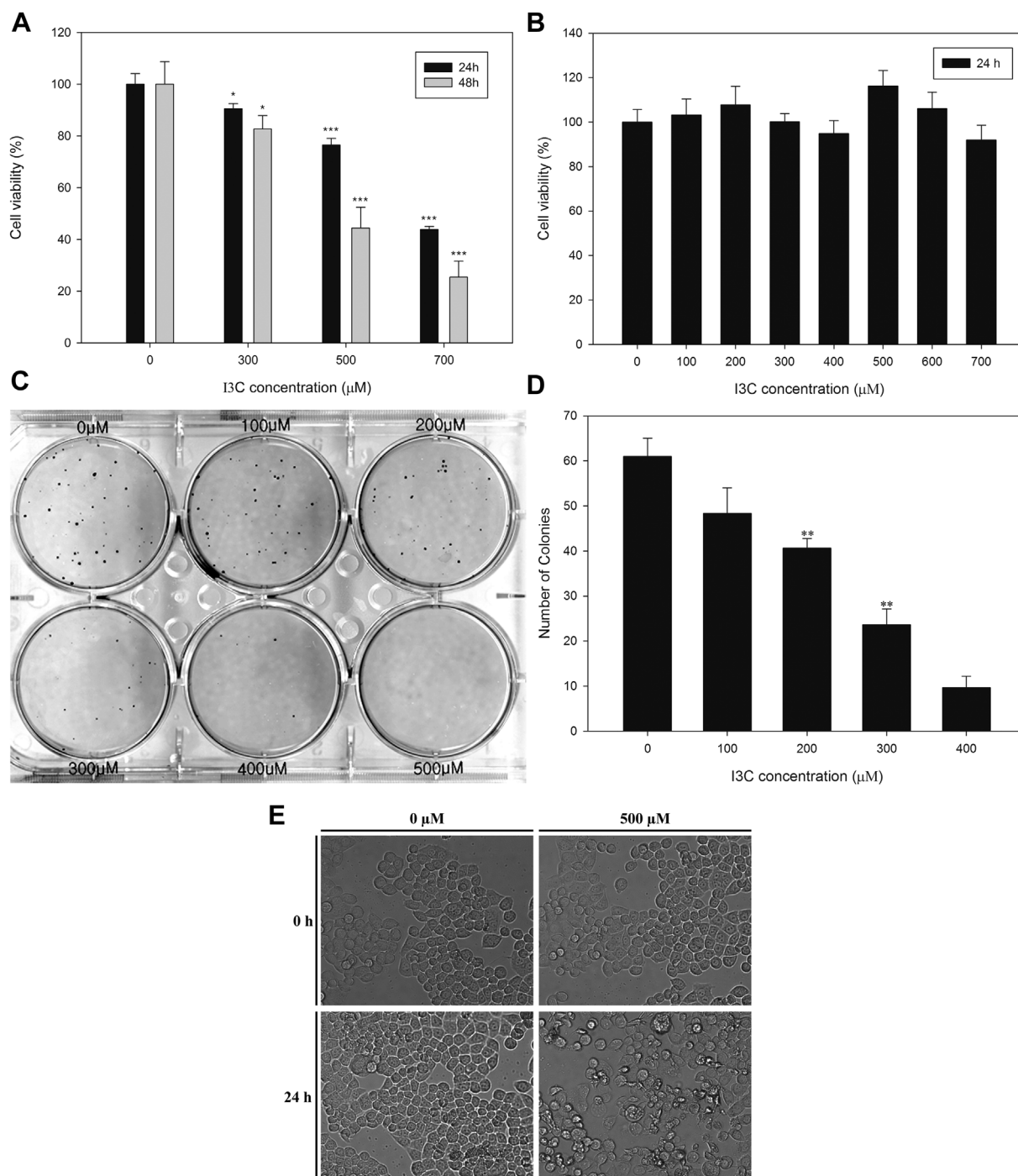


Fig. 1. Cell viability and proliferation of I3C-treated Huh-7 cells. (A) Viability was measured by the MTT assay. The results showed that I3C has dose- and time-dependent anti-proliferation effects. Each bar represents mean \pm SEM. Single and triple asterisks indicate significant differences from the control cells (* $p < 0.05$ and *** $p < 0.001$, respectively). (B) Viability was measured by the MTT assay in I3C-treated WRL 68 cells. (C) Effects of I3C on the colony formation ability of Huh-7 cells. We observed that the number of colonies was decreased by incubation in a dose-dependent manner. (D) The number of colonies in the different concentration of I3C-treated plates. Each bar represents mean \pm SEM. Single and triple asterisks indicate significant differences from the control cells (* $p < 0.05$, ** $p < 0.01$ and *** $p < 0.001$, respectively). (E) Morphological changes in 500 μM I3C-treated Huh-7 cells.

inhibited by up to 50% following treatment with 500 μM I3C for 48 h. We also conducted MTT assays in normal human hepatocyte WRL68 cells (Fig. 1B). I3C decreased the viability of WRL68 to 92% at a concentration of 700 μM . We found that I3C showed little cytotoxic effect against WRL68 cells. Moreover, markedly fewer colonies were produced by I3C-treated cells than control cells (Fig. 1C and D). Furthermore, we observed that 500 μM of I3C treatment for 24 h induced detectable morphological changes in Huh-7 cells (Fig. 1E). Our results

suggested that I3C inhibited the growth and survival of Huh-7 cells in dose- and time-dependent manners.

3.2. I3C induced apoptosis in Huh-7 cells

We next performed an Annexin V/PI double-staining assay to investigate I3C-induced apoptosis in Huh-7 cells. We stained Huh-7 cells with Annexin V and PI dye after treatment with different concentration

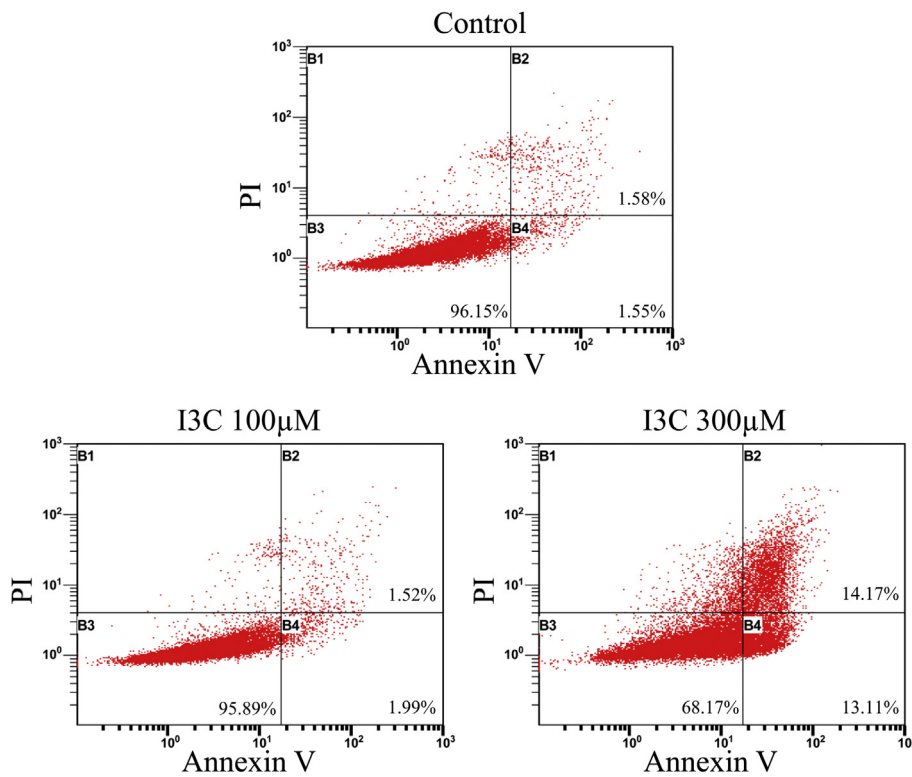


Fig. 2. FACS analysis of Annexin-V and PI double-stained Huh-7 cells. Huh-7 cells were treated with 0, 100, 300, and 500 μ M I3C for 24 h and then stained with Annexin-V and PI to assess apoptotic cells by FACS analysis. I3C induced apoptosis in a concentration-dependent manner. The proportions of apoptotic cells (upper and lower right) are shown.

of I3C (0, 100 and 300 μ M) for 24 h. Subsequently, the cells were analyzed by flow cytometry. Our results showed that the levels of Annexin V+/PI- and Annexin V+/PI+ -marked cells were increased by I3C treatment in a dose-dependent manner (Fig. 2). The percentage of total apoptotic cells (both early and late apoptosis) was 3.09% in the control group, whereas the percentages of apoptotic cells in the groups treated with 100 μ M and 300 μ M I3C were 3.45% and 25.33%, respectively. Our results demonstrated that I3C induces apoptosis in Huh-7 cells.

3.3. I3C induced DNA fragmentation in Huh-7 cells

To confirm I3C-induced DNA fragmentation in Huh-7 cells, TUNEL assay was performed. Huh-7 cells were treated with 0, 100, 300, and 500 μ M I3C for 24 h. Then, the I3C-treated and control Huh-7 cells were analyzed by the TUNEL assay. I3C-treatment of Huh-7 cells induced a dose-dependent increase in fluorescence (Fig. 3).

3.4. I3C induced overexpression of Hsp27

The differentially expressed proteins between control and 500 μ M I3C-treated Huh-7 cells for 24 h were detected by 2-DE. Proteins were separated horizontally by PI and vertically by molecular weight (Fig. 4). We detected that four spots (proteins) were increased in 500 μ M I3C-treated cells when compared to the levels in control cells. We identified these four proteins by MALDI-TOF (Table 1). One of them was Hsp27 protein. We confirmed that I3C treatment increased Hsp27 expression in Huh-7 cells by performing western blotting (Fig. 5A). Bar graph showed the relative expression level of Hsp27 (Fig. 5B). We investigated the role of Hsp27. The major function of Hsp27 in cells is to regulate apoptosis (Concannon et al., 2003b).

3.5. I3C activated apoptosis-related proteins and changed the level of Akt, ERK expression

We next examined the expression of proteins involved in apoptosis. After treatment with different concentration of I3C in Huh-7 cells for

24 h and 48 h, the levels of PARP, p53, caspase-3, -7, -9 expressions were measured by western blotting (Fig. 6A and Fig. 6C). Bar graphs showed the relative expression levels of each protein (Fig. 6B and D). The results showed that I3C treatment markedly up-regulated the expression of cleaved PARP and cleaved caspase-3, -7, -9, which are hallmarks of apoptosis. Moreover Akt, ERK and JNK signaling pathways were analyzed by western blotting. We observed that Akt level was consistent, whereas pAkt and MDM2 expression level was increased (Fig. 7A). p53 is tumor suppressor protein and it is regulated by Akt and MDM2 (Ogawara et al., 2002). We analyzed ERK signaling pathway (Fig. 7B). We found that the level of ERK expression level was consistent. On contrary, pERK expression level was decreased. bad protein is regulated by ERK (Shen et al., 2010). We detected degradation of bad and bid, whereas increase of pbad. We also analyzed JNK signaling pathways (Fig. 7C). The level of pJNK expression level was slightly decreased. However, there was no significant changes in JNK, and p38 expression levels. Bar graphs showed the relative expression lsevels of each protein (Fig. 7D).

3.6. Hsp27 knockdown increased viability in Huh-7 cells

To demonstrate the anti-proliferation effect of Hsp27 induced by I3C, Huh-7 cells were transfected with control-siRNA and Hsp27-siRNA. Huh-7 cells were seeded at 96 plates at a density of 3×10^3 cells per well. After then, the cells were treated with 500 μ M I3C and DMSO for 24 h. Subsequently, 10 μ L of EZ-Cytotoxicity was treated in each well and incubated for 1 h under standard conditions. We measured the level of formazan using a spectrophotometer at 450 nm. We compared the viability of Control-siRNA transfected group and Hsp27-siRNA transfected group. Hsp27-siRNA transfected Huh-7 cells showed higher viability than those of control-siRNA. Our results indicated that Hsp27 knockdown increased viability in Huh-7 cells (Fig. 8A).

3.7. Hsp27 induced PARP cleavage and DNA fragmentation

We investigated the relationship between inhibition of Hsp27 and

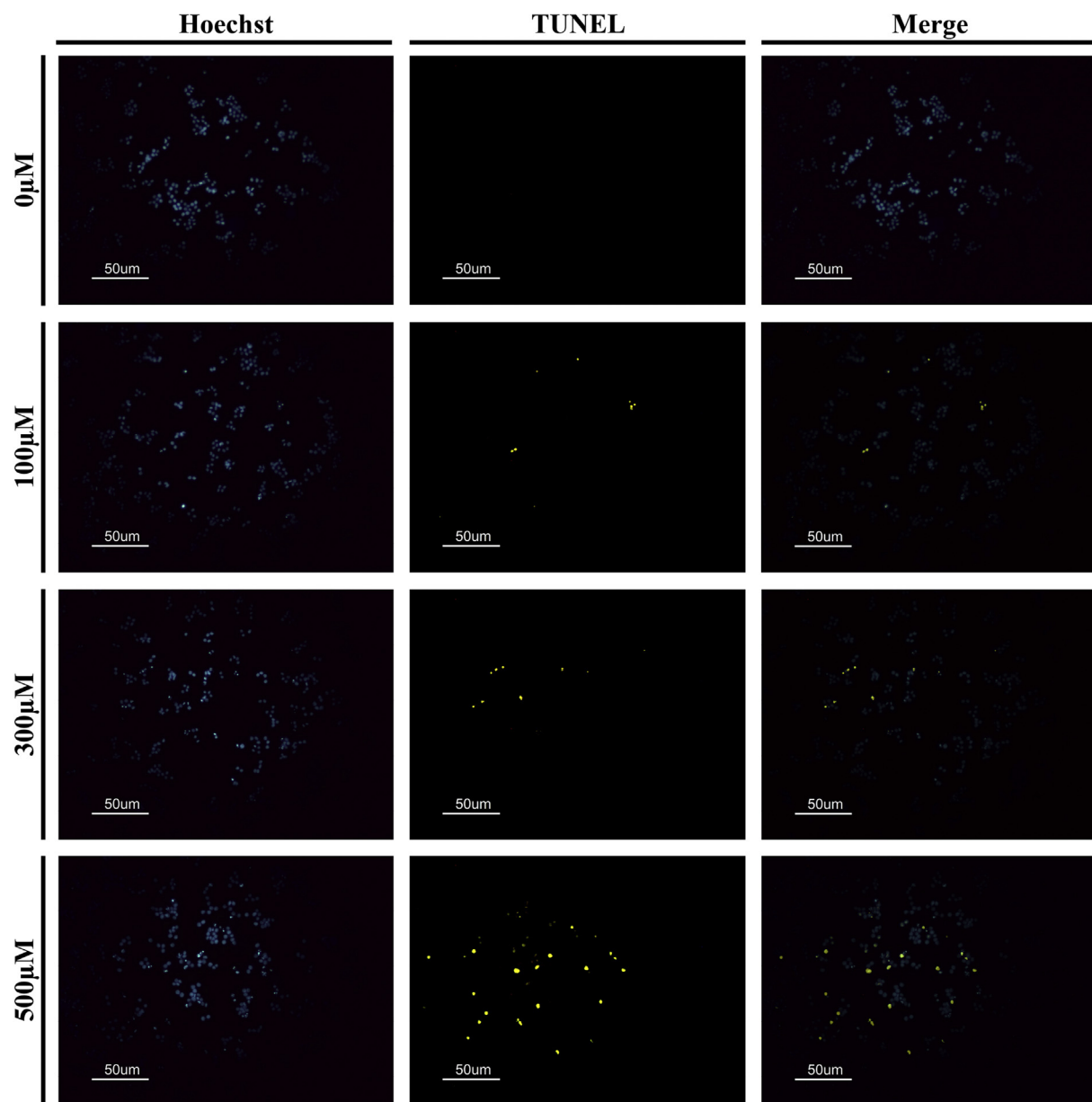


Fig. 3. Detection of DNA fragmentation in apoptotic cells using TUNEL assay. Huh-7 cells were treated with 0, 100, 300, and 500 μ M I3C for 24 h, and then DNA fragmentation was visualized by fluorescence microscopy (100 \times). Blue fluorescence is nuclei; green fluorescence is DNA fragmentation. The merged images show blue-stained nuclei with green-stained nicked DNA. (For interpretation of the references to colour in this figure legend, the reader is referred to the Web version of this article.)

apoptotic proteins, such as caspase-3, -7, -9 and PARP (Fig. 8B and C). Huh-7 cells were transfected with control-siRNA or Hsp27-siRNA for 4 h. After 4 h, media was changed into complete media (containing 10% FBS, 1% antibiotics). After 44 h and subsequently, the transfected cells were treated with 500 μ M I3C or control (DMSO) for 24 h and cell lysates were analyzed by western blotting (PARP, cleaved PARP, caspase-3, -7, -9, cleaved caspase-7, -9, and Hsp27). Compared to the control-siRNA transfected group, Hsp27-siRNA transfected group showed the decrease of cleaved PARP in the 500 μ M I3C treated group. We also detected that inhibition of Hsp27 decreased DNA fragmentation (Fig. 8D). These results suggested that Hsp27 is related to DNA fragmentation.

3.8. Hsp27 knockdown inhibited apoptosis in Huh-7 cells

We performed an Annexin V/Pi double-staining assay to investigate

I3C-induced apoptosis in control-siRNA and Hsp27-siRNA transfected Huh-7 cells. Huh-7 cells were transfected with control-siRNA or Hsp27-siRNA for 4 h. After 4 h, media was changed into complete media (containing 10% FBS, 1% antibiotics). After 44 h, cells were treated with I3C (300 or 500 μ M) or control (DMSO) for 24 h. Subsequently, we stained the cells with Annexin V and PI dye and analyzed the cells by flow cytometry. Our results showed that the levels of Annexin V+ /PI- and Annexin V+ /PI+ - marked cells were decreased in I3C-treated and Hsp27-siRNA transfected Huh-7 cells compared to the control (I3C-treated and control-siRNA transfected cells). In 300 μ M I3C-treated group, the percentage of total apoptotic cells (both early and late apoptosis) was 22.09% in control-siRNA transfected cells, whereas the percentage of apoptotic cells in Hsp27-siRNA transfected group was 12.84% (Fig. 9A). Moreover, in 500 μ M I3C treated group, the percentage of total apoptotic cells was 35.84% in Control-siRNA transfected cells, whereas the percentage of apoptotic cells in Hsp27-siRNA

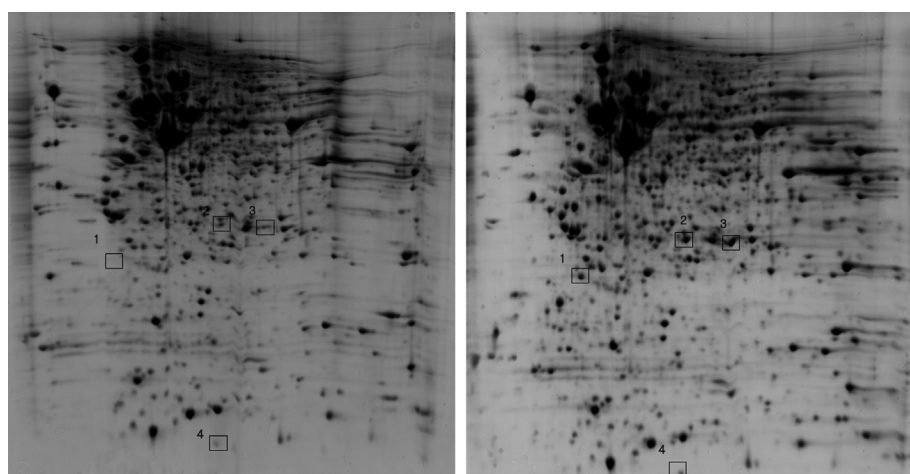


Fig. 4. Visualization of differentially expressed proteins between untreated control and 500 μ M I3C-treated Huh-7 cells by 2-DE. After 24 h of treatment with 500 μ M I3C, total proteins in the cells were extracted and separated according to PI and molecular weight. Separated proteins were visualized by Coomassie blue staining. Differentially expressed proteins are numbered and shown in rectangular boxes. We analyzed the differentially expressed proteins by MALDI-TOF, and the results are shown in Table 1.

transfected group was 28.5%. Bar graphs showed the relative number of apoptotic cells (Fig. 9B). Our results demonstrated that inhibition of Hsp27 suppressed apoptosis induced by I3C in Huh-7 cells.

4. Discussion

Liver cancer is one of the most common cancers in the world, and conventional therapies, such as chemotherapy, radiation, and surgery, offer poor treatment options. This is why many researchers have struggled to discover alternative methods to cure liver cancer. The objective of our study was to identify effective anti-cancer agents. I3C is a phytochemical found in many vegetables, such as kale, sprouts, and cabbage (Sherer et al., 2017), and it is known that I3C inhibits the proliferation of many cancers, including human breast, colon, and prostate cancers (Bai et al., 2013). The mechanism underlying I3C-induced apoptosis is likely to be multifactorial. I3C suppressed human reproductive cancer cells by inducing G1 cell cycle arrest (Hsu et al., 2006), whereas I3C induced apoptosis in human prostate cancer cells through a p53-, bcl-2-, and bax-independent signaling pathway (Nachshon-Kedmi et al., 2003).

The effects of I3C on liver carcinoma cells have not been previously investigated. In this study, we examined the anti-cancer effects of I3C in the human hepatocellular carcinoma Huh-7 cells. To understand the mechanism of I3C-induced apoptosis in Huh-7 cells, we performed apoptosis-related assays, 2-DE, and western blotting.

Caspases are a family of protease enzymes which play important roles in programmed cell death, such as apoptosis and inflammation. Activated caspases induced the degradation of cellular components and carry out programmed cell death with minimal influence on surrounding tissues and cells (Rathore et al., 2015). Caspase-3 is a member of caspase family; frequently catalyzed the specific cleavage of proteins and it induced cell death (Rogers et al., 2017). Caspase-7 is also one of caspase proteins and highly related to caspase-3 (Flanagan et al., 2016). Activated caspase-3 and -7 cleave substrates, ultimately inducing the morphological and biochemical hallmarks of apoptosis, such as

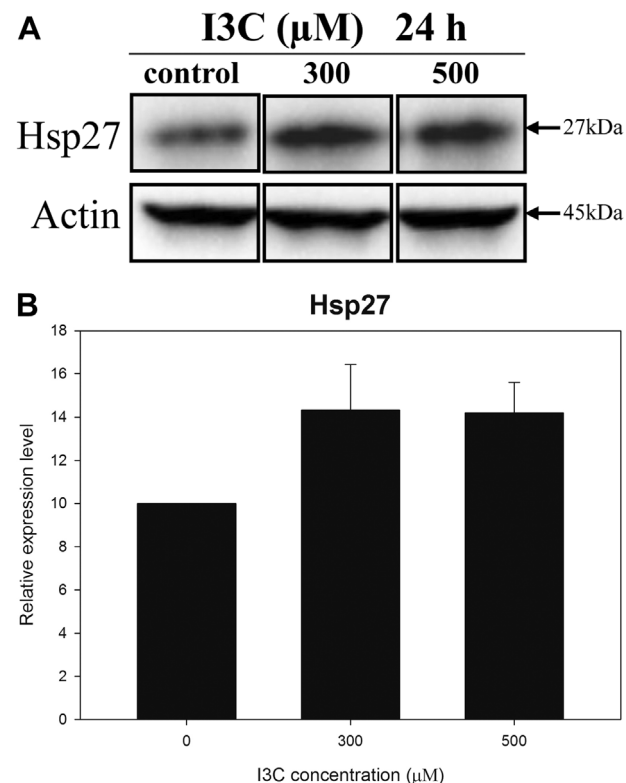


Fig. 5. (A) Western blot analysis of Hsp27 in I3C-treated Huh-7 cells. The cells were treated with 0, 300, and 500 μ M I3C for 24 h. (B) Bar graph showed the relative value of Hsp27 expression after treatment of I3C for 24 h in Huh-7 cells. The relative expression levels were normalized to β -actin.

exposure of phosphatidylserine, condensation of nuclear and DNA fragmentation (Lamkanfi and Kanneganti, 2010). Caspase-9 is an

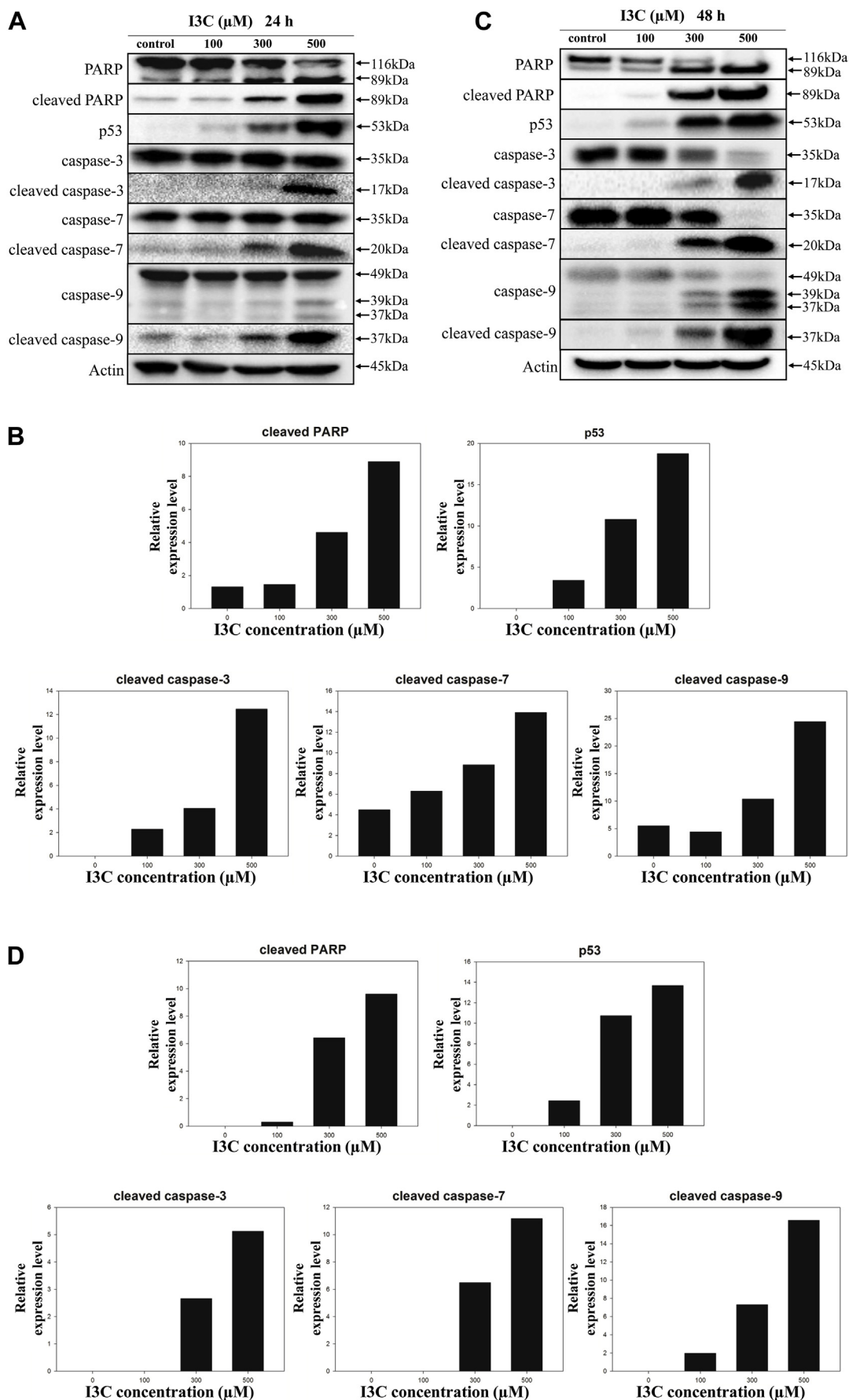
Table 1
Identification of differentially expressed protein spots in the control and I3C-treated groups in Huh-7 cells.

Spot no. ^a	Protein name	Protein function	Accession no. ^b	Sequence cov. (%) ^c	Theoretical Mw(Da)/PI	Expression
1	Coiled-coil Domain-containing Protein 27	circulatory function	Q2M243	1	75,821/5.53	+
2	Heat Shock Protein beta-1	regulating apoptosis	P04792	61	22,826/5.98	+
3	Osteocalcin	metabolic regulation	P40147	10	11,022/5.23	+
4	Eukaryotic Translation Initiation factor 5A-1	Translation initiation	P63241	20	17,049/5.08	+

^a Spot number on 2-DE gel.

^b Swiss-Prot accession numbers.

^c Sequence coverage.



(caption on next page)

Fig. 6. Western blot analysis of PARP, p53, caspase-3, -7, -9 and cleaved PARP, cleaved caspase-3, -7, -9 in I3C-treated Huh-7 cells. Huh-7 cells were seeded into a culture dish and incubated for 24 h, and then treated with 0, 100, 300, and 500 μ M I3C for 24 and 48 h. The expression of PARP, p53 and caspase-3, -7, -9 as well as cleaved PARP, cleaved caspase-3, -7, -9 in Huh-7 cells was analyzed after 24 h (A) and 48 h (C) of I3C treatment. Bar graphs showed the relative value of PARP, p53, cleaved caspase-3, -7, -9 proteins after treatment of I3C for 24 h (B) and 48 h (D) in Huh-7 cells. The relative expression levels were normalized to β -actin.

essential factor initiating apoptosis signal transduction and forming apoptosome (Wurster et al., 2012). In this study, we investigated caspase-3, -7 and -9 activity following treatment of I3C in Huh-7 cells. Our results showed that I3C induced cleavage of caspase-3, -7 and -9 (Fig. 6A and C).

PARP involved in several cellular processes, such as DNA repair and programmed cell death (Luo et al., 2017). Cleavage of PARP by caspases is an important event during execution of apoptosis (Gowda Saralmama et al., 2018). We also studied PARP activity following treatment of I3C in Huh-7 cells. Our results showed that I3C induced cleavage of PARP (Fig. 6A and C).

p53 is a tumor suppressor protein and it prevents formation of cancer (Surget et al., 2013). It is well known that mutations of p53 gene are the most common genetic alterations in various human tumors (Levine et al., 1991). In our experiment, we detected the overexpression of p53 in I3-treated Huh-7 cells (Fig. 6A and C). p53 is regulated by Akt and MDM2 signaling pathways (Gottlieb et al., 2002). There is an auto regulatory feedback loop connection between p53 and MDM2. p53

activates MDM2 expression; MDM2, in turn suppress p53 activity (Moll and Petrenko, 2003). Our results showed that cleaved MDM2 and p53 expression levels were increased in a dose-dependent manner (Fig. 6A, C and 7A).

The Ras/Raf/MEK (mitogen-activated protein kinase/ERK kinase)/ERK (extracellular-signal-regulated kinase) pathway is a signaling system regulating cell proliferation and survival (Kolch, 2000). ERK signaling pathway regulates pro-apoptotic protein bad (Ellert-Miklaszewska et al., 2005). We investigated ERK and bad protein expression level. Generally, bad expression level is consistent, whereas pbad is decreased (Dong et al., 2007; Fernando and Wimalasena, 2004; Liang et al., 2012; Liu et al., 2012; Pancholi et al., 2008). Phosphorylated bad is sequestered by 14-3-3 and other molecules and it leads to cell survival, whereas total bad was integrated with mitochondria and it induces release of cytochrome c to the cytoplasm followed by PARP cleavage, DNA fragmentation and Cell shrinkage (Fernando and Wimalasena, 2004). However, our results showed that the level of bad was decreased and pbad (ser112) was increased (Fig. 7B). We conclude

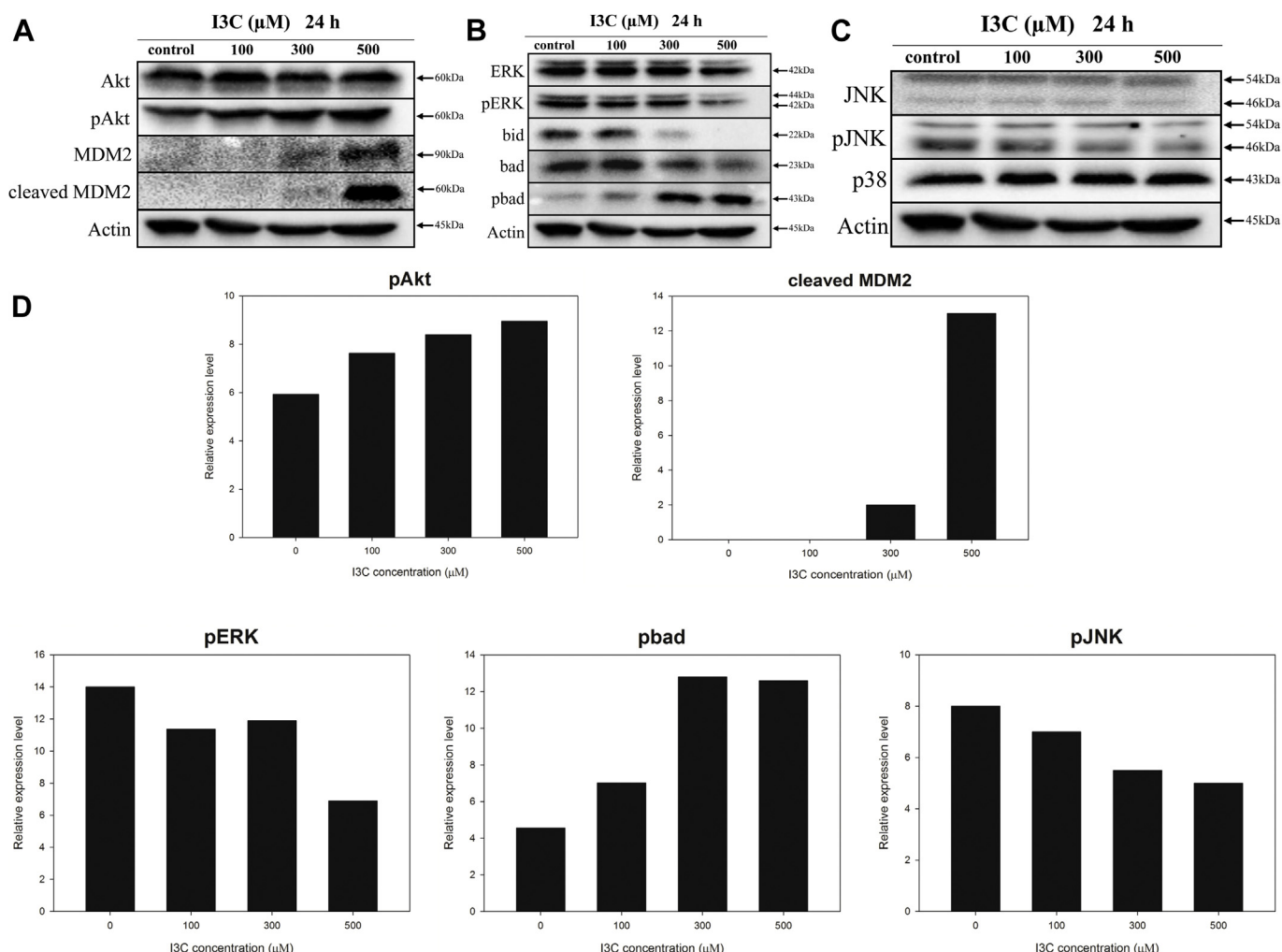
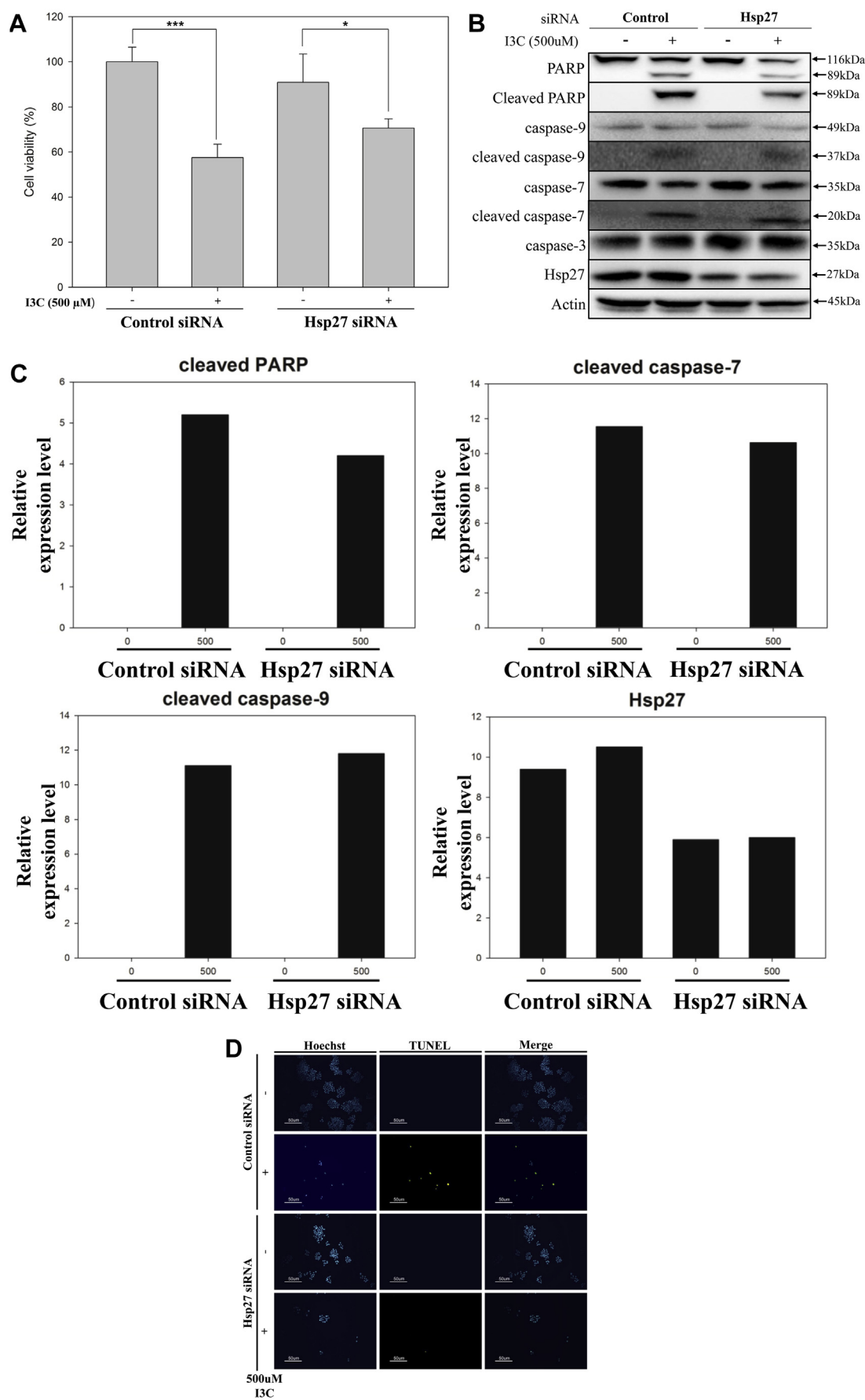


Fig. 7. Western blot analysis of Akt, JNK and ERK signaling pathways in I3C-treated Huh-7 cells. (A) We analyzed the level of Akt, pAkt and MDM2 expression. (B) The level of ERK, pERK, bid, bad, pbad expression was analyzed. (C) The level of JNK, pJNK, p38 expression was analyzed. (D) Bar graphs showed the relative value of pAkt, cleaved MDM2, pERK, pbad, and pJNK expression level after treatment of I3C for 24 h in Huh-7 cells. The relative expression levels were normalized to β -actin.



(caption on next page)

Fig. 8. Inhibition Hsp27 through transfection of Hsp27-siRNA in Huh-7 cells. Huh-7 cells were transfected with control-siRNA or Hsp27-siRNA for 48 h. The transfected cells were treated with I3C (500 μ M) or control (DMSO) for 24 h. (A) Cell viability was measured by WST-1 assay. Inhibition of Hsp27 increased the cell viability. Each bar represents mean \pm SEM. Single and triple asterisks indicate significant differences from the control cells (at * p < 0.05 and *** p < 0.001, respectively). (B) Western blotting in control or Hsp27-siRNA transfected Huh-7 cells. Inhibition of Hsp27 induced inactivation of PARP protein. (C) Bar graphs showed the relative value of cleaved PARP, cleaved caspase-7, -9 and Hsp27 expression. The relative expression levels were normalized to β -actin. (D) TUNEL assay was performed to visualize DNA fragmentation. Blue fluorescence is nuclei; green fluorescence is DNA fragmentation. The merged images show blue-stained nuclei with green-stained nicked DNA. (For interpretation of the references to colour in this figure legend, the reader is referred to the Web version of this article.)

that the mechanism of pro-apoptotic protein bad-related apoptosis in I3C-treated Huh-7 cells is unclear. We also examined the JNK signaling pathway through western blotting (Fig. 7C). However, there is no significant change in JNK signaling activation.

Differentially expressed proteins between control and 500 μ M I3C-treated Huh-7 cells were identified by 2-DE. Four spots that showed a significant change in expression were chosen and identified by MALDI-TOF. One of them is Hsp27, which is regarded as an apoptosis-related protein (Fig. 4 and Table 1). We validated the 2-DE proteomic analysis results by western blotting (Fig. 5A). Our results showed that treatment of I3C in Huh-7 cells increased the level of Hsp27 expression.

Hsp27 is encoded by the *HSPB1* gene (Carper et al., 1990; Hunt et al., 1997) and is a chaperone of the small heat shock protein (sHsp)

group. Generally, sHsps function as chaperones, regulate cell growth, and inhibit apoptosis. A major function of Hsp27 is maintaining cell survival under stress conditions. Hsp27 is also involved in an apoptotic signaling pathway, and many studies have shown that Hsp27 inhibits apoptosis. Hsp27 interacts with the outer mitochondrial membrane and inhibits the activation of apoptotic factors, such as cytochrome c, Apaf-1, and the dATP complex, and inhibits activation of procaspase-9 (Sarto et al., 2000). Hsp27 also regulates apoptosis by controlling Akt activation (Rane et al., 2003) and inhibiting various apoptotic stimuli (Wang et al., 2014; Tian et al., 2016; Chen et al., 2016). One mechanism through which Hsp27 inhibits apoptosis is by preventing cytosol cytochrome c from binding to Apaf-1 (Bruey et al., 2000; Garrido et al., 1999). Hsp27 was also shown to inhibit Daxx- and ASK1-

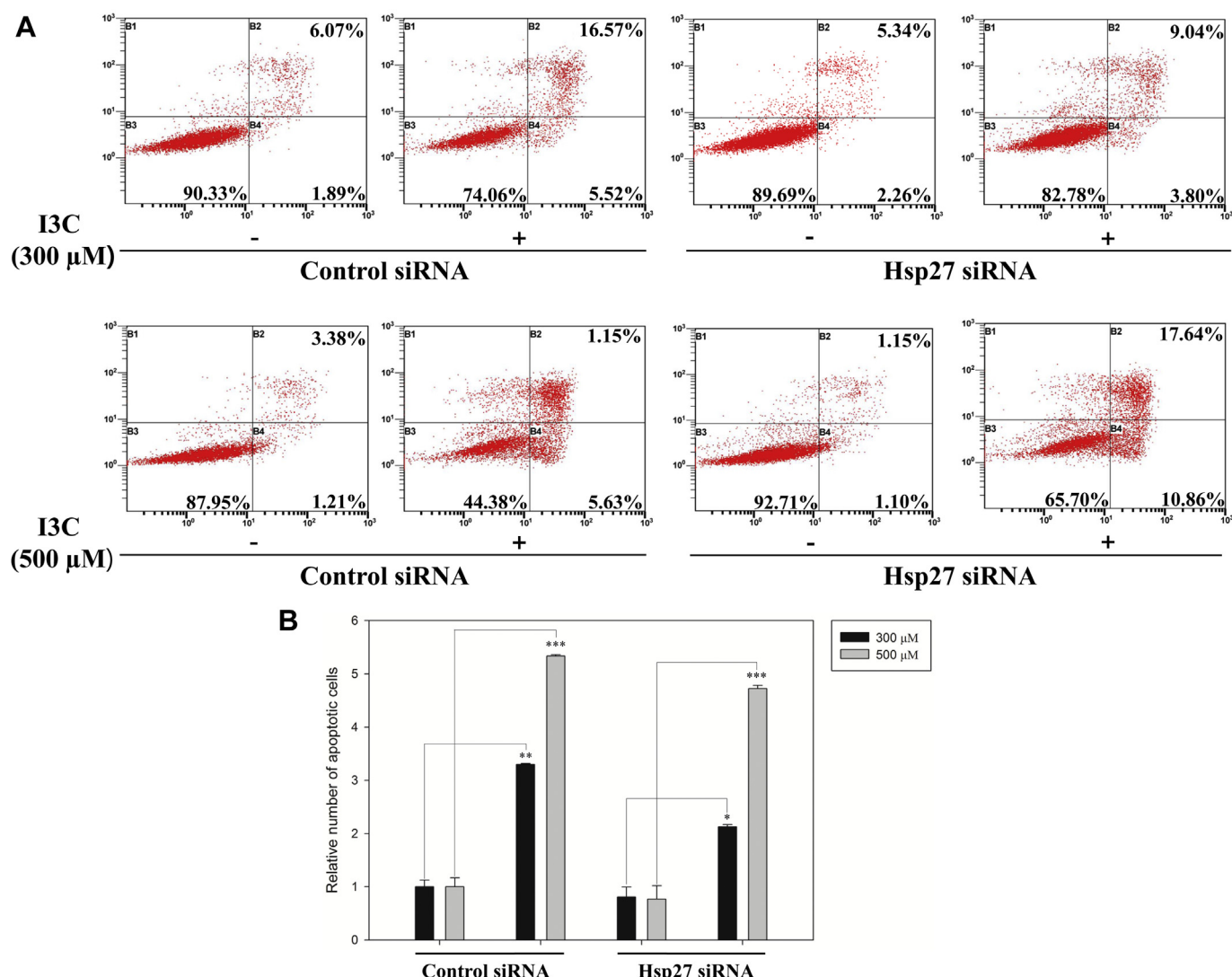


Fig. 9. FACS analysis in control or Hsp27-transfected Huh-7 cells. Huh-7 cells were transfected with control-siRNA or Hsp27-siRNA for 48 h. The transfected cells were treated with I3C (300 μ M or 500 μ M) or control (DMSO) for 24 h. (A) The cells were stained with Annexin-V and PI to assess apoptotic cells by FACS analysis. Hsp27 induced apoptosis in Huh-7 cells. (B) Relative number of Apoptotic cells. Each bar represents mean \pm SEM. Single and triple asterisks indicate significant differences from the control cells (* p < 0.05, ** p < 0.01 and *** p < 0.001, respectively).

dependent apoptosis (Charette et al., 2000).

However, few studies have shown that Hsp27 can induce apoptosis in human cells. For example, overexpression of Hsp27 induced cell cycle arrest and apoptosis in pancreatic cancer cells (Guo et al., 2015). The study showed that Hsp27 acts as a pro-apoptotic factor in pancreatic cancer cells. In our study, we demonstrated that the Hsp27 expression level increased as apoptosis progressed. Our results showed that inhibition of Hsp27 increased the viability of I3C-treated Huh-7 cells by WST-1 assay. We also detected that inhibition of Hsp27 suppressed apoptosis by FACS analysis. However, our results suggested that there are no significant variations in caspase-3, -7, and -9 in Hsp27-siRNA transfected Huh-7 cells. But, we observed inactivation of PARP cleavage in Hsp27-siRNA transfected Huh-7 cells. It is known that PARP cleavage induces DNA fragmentation and apoptosis (Agarwal et al., 2009). TUNEL assay results showed that DNA fragmentation was inhibited in Hsp27-siRNA transfected Huh-7 cells compared to control. Taken together, we concluded that I3C may play a crucial role in regulation of PARP cleavage and DNA fragmentation.

We also detected apoptotic pathway activation following treatment with I3C. Our results showed that the p53 expression level was increased. We also observed activation of caspase-3, -7, -9, and PARP by I3C treatment. There are many studies showing that activation of the caspase pathway induces apoptosis (Dantas et al., 2014; Khazaei et al., 2017; Mondal and Bennett, 2016), likewise, cleavage of PARP also induces apoptosis (Vizotto-Duarte et al., 2016). However, Even though we demonstrated that Hsp27 induced apoptosis in Huh-7 cells, it is unclear which Hsp27 mechanisms were involved in I3C-induced apoptosis because Hsp27 has many functions when it comes to apoptosis (Concannon et al., 2003a).

5. Conclusion

In summary, our study showed that I3C induced apoptosis in human hepatocellular carcinoma Huh-7 cells. Through transfection experiments, we concluded that Hsp27 is an important mediator of I3C-induced apoptosis in Huh-7 cells. Moreover, treatment of Huh-7 cells with I3C activated proteins involved in various apoptotic signaling pathways, such as PARP, caspase-3, -7, -9, and p53.

Acknowledgements

The present study was supported by a grant from the Business for Cooperative R&D between Industry, Academy, and Research Institutes (Grant no. C0443066) funded by the Korean Small and Medium Business Administration in 2016 and the Basic Science Research Program through the National Research Foundation of Korea funded by the Ministry of Education, Science and Technology (NRF-2014R1A6A3A04054307).

Transparency document

Transparency document related to this article can be found online at <http://dx.doi.org/10.1016/j.fct.2018.05.014>.

References

- Agarwal, A., Mahfouz, R.Z., Sharma, R.K., Sarkar, O., Mangrola, D., Mathur, P.P., 2009. Potential biological role of poly (ADP-ribose) polymerase (PARP) in male gametes. *Reprod. Biol. Endocrinol.* 7, 143.
- Bai, L.Y., Weng, J.R., Chiu, C.F., Wu, C.Y., Yeh, S.P., Sargeant, A.M., Lin, P.H., Liao, Y.M., 2013. OSU-A9, an indole-3-carbinol derivative, induces cytotoxicity in acute myeloid leukemia through reactive oxygen species-mediated apoptosis. *Biochem. Pharmacol.* 86, 1430–1440.
- Bruey, J.M., Ducasse, C., Bonniaud, P., Ravagnan, L., Susin, S.A., Diaz-Latoud, C., Gurbuxani, S., Arrigo, A.P., Kroemer, G., Solary, E., Garrido, C., 2000. Hsp27 negatively regulates cell death by interacting with cytochrome c. *Nat. Cell Biol.* 2, 645–652.
- Carper, S.W., Rocheleau, T.A., Storm, F.K., 1990. cDNA sequence of a human heat shock protein HSP27. *Nucleic Acids Res.* 18, 6457.
- Charette, S.J., Lavoie, J.N., Lambert, H., Landry, J., 2000. Inhibition of Daxx-mediated apoptosis by heat shock protein 27. *Mol. Cell Biol.* 20, 7602–7612.
- Chen, X., Dong, X.S., Gao, H.Y., Jiang, Y.F., Jin, Y.L., Chang, Y.Y., Chen, L.Y., Wang, J.H., 2016. Suppression of HSP27 increases the antitumor effects of quercetin in human leukemia U937 cells. *Mol. Med. Rep.* 13, 689–696.
- Choi, H.S., Cho, M.C., Lee, H.G., Yoon, D.Y., 2010. Indole-3-carbinol induces apoptosis through p53 and activation of caspase-8 pathway in lung cancer A549 cells. *Food Chem. Toxicol.* 48, 883–890.
- Concannon, C.G., Gorman, A.M., Samali, A., 2003a. On the role of Hsp27 in regulating apoptosis. *Apoptosis* 8, 61–70.
- Concannon, C.G., Gorman, A.M., Samali, A., 2003b. On the role of Hsp27 in regulating apoptosis. *Apoptosis* 8, 61–70.
- Dantas, A.E., Horta, C.C., Martins, T.M., Do Carmo, A.O., Mendes, B.B., Goes, A.M., Kalapothakis, E., Gomes, D.A., 2014. Whole venom of *Loxosceles similis* activates caspases-3, -6, -7, and -9 in human primary skin fibroblasts. *Toxicon* 84, 56–64.
- Demaria, S., Golden, E.B., Formenti, S.C., 2015. Role of local radiation therapy in cancer immunotherapy. *JAMA Oncol.* 1, 1325–1332.
- Dong, S., Kang, S., Gu, T.L., Kardar, S., Fu, H., Lonial, S., Khouri, H.J., Khuri, F., Chen, J., 2007. 14-3-3 Integrates prosurvival signals mediated by the AKT and MAPK pathways in ZNF198-FGR1-transformed hematopoietic cells. *Blood* 110, 360–369.
- Ellert-Miklaszewska, A., Kaminska, B., Konarska, L., 2005. Cannabinoids down-regulate PI3K/Akt and Erk signalling pathways and activate proapoptotic function of Bad protein. *Cell. Signal.* 17, 25–37.
- Fernando, R.I., Wimalasena, J., 2004. Estradiol abrogates apoptosis in breast cancer cells through inactivation of BAD: Ras-dependent nongenomic pathways requiring signaling through ERK and Akt. *Mol. Biol. Cell* 15, 3266–3284.
- Flanagan, L., Meyer, M., Fay, J., Curry, S., Bacon, O., Duessmann, H., John, K., Boland, K.C., McNamara, D.A., Kay, E.W., Bantel, H., Schulze-Bergkamen, H., Prehn, J.H., 2016. Low levels of Caspase-3 predict favourable response to 5FU-based chemotherapy in advanced colorectal cancer: caspase-3 inhibition as a therapeutic approach. *Cell Death Dis.* 7, e2087.
- Garrido, C., Bruey, J.M., Fromentin, A., Hammann, A., Arrigo, A.P., Solary, E., 1999. HSP27 inhibits cytochrome c-dependent activation of procaspase-9. *Faseb J.* 13, 2061–2070.
- Gottlieb, T.M., Leal, J.F., Seger, R., Taya, Y., Oren, M., 2002. Cross-talk between Akt, p53 and Mdm2: possible implications for the regulation of apoptosis. *Oncogene* 21, 1299–1303.
- Gowda Saralamma, V.V., Lee, H.J., Raha, S., Lee, W.S., Kim, E.H., Lee, S.J., Heo, J.D., Won, C., Kang, C.K., Kim, G.S., 2018. Inhibition of IAP's and activation of p53 leads to caspase-dependent apoptosis in gastric cancer cells treated with Scutellarein. *Oncotarget* 9, 5993–6006.
- Guo, Y., Ziesch, A., Hocke, S., Kampmann, E., Ochs, S., De Toni, E.N., Goke, B., Gallmeier, E., 2015. Overexpression of heat shock protein 27 (HSP27) increases gemcitabine sensitivity in pancreatic cancer cells through S-phase arrest and apoptosis. *J. Cell Mol. Med.* 19, 340–350.
- Hsu, J.C., Dev, A., Wing, A., Brew, C.T., Bjeldanes, L.F., Firestone, G.L., 2006. Indole-3-carbinol mediated cell cycle arrest of LNCaP human prostate cancer cells requires the induced production of activated p53 tumor suppressor protein. *Biochem. Pharmacol.* 72, 1714–1723.
- Hunt, C.R., Goswami, P.C., Kozak, C.A., 1997. Assignment of the mouse Hsp25 and Hsp105 genes to the distal region of chromosome 5 by linkage analysis. *Genomics* 45, 462–463.
- Khazaei, S., Ramachandran, V., Abdul Hamid, R., Mohd Esa, N., Etemad, A., Moradiopoor, S., Ismail, P., 2017. Flower extract of *Allium sativum* triggered apoptosis, activated caspase-3 and down-regulated antiapoptotic Bcl-2 gene in HeLa cancer cell line. *Biomed. Pharmacother.* 89, 1216–1226.
- Kim, J.Y., Jeon, Y.K., Jeon, W., Nam, M.J., 2010. Fisetin induces apoptosis in Huh-7 cells via downregulation of BIRC8 and Bcl2L2. *Food Chem. Toxicol.* 48, 2259–2264.
- Kolch, W., 2000. Meaningful relationships: the regulation of the Ras/Raf/MEK/ERK pathway by protein interactions. *Biochem. J.* 351 (Pt 2), 289–305.
- Lamkanfi, M., Kanneganti, T.D., 2010. Caspase-7: a protease involved in apoptosis and inflammation. *Int. J. Biochem. Cell Biol.* 42, 21–24.
- Lasley, F.D., Mannina, E.M., Johnson, C.S., Perkins, S.M., Althouse, S., Maluccio, M., Kwo, P., Cardenes, H., 2015. Treatment variables related to liver toxicity in patients with hepatocellular carcinoma, Child-Pugh class A and B enrolled in a phase 1-2 trial of stereotactic body radiation therapy. *Pract Radiat Oncol* 5, e443–449.
- Levine, A.J., Momand, J., Finlay, C.A., 1991. The p53 tumour suppressor gene. *Nature* 351, 453–456.
- Liang, R.R., Zhang, S., Qi, J.A., Wang, Z.D., Li, J., Liu, P.J., Huang, C., Le, X.F., Yang, J., Li, Z.F., 2012. Preferential inhibition of hepatocellular carcinoma by the flavonoid Baicalein through blocking MEK-ERK signaling. *Int. J. Oncol.* 41, 969–978.
- Lin, H., Gao, X., Chen, G., Sun, J., Chu, J., Jing, K., Li, P., Zeng, R., Wei, B., 2015. Indole-3-carbinol as inhibitors of glucocorticoid-induced apoptosis in osteoblastic cells through blocking ROS-mediated Nrf2 pathway. *Biochem. Biophys. Res. Commun.* 460, 422–427.
- Liu, Y., Sun, S.Y., Owonikoko, T.K., Sica, G.L., Curran, W.J., Khuri, F.R., Deng, X., 2012. Rapamycin induces Bad phosphorylation in association with its resistance to human lung cancer cells. *Mol. Canc. Therapeut.* 11, 45–56.
- Luo, H., Liang, H., Chen, J., Xu, Y., Chen, Y., Xu, L., Yun, L., Liu, J., Yang, H., Liu, L., Peng, J., Liu, Z., Tang, L., Chen, W., Tang, H., 2017. Hydroquinone induces TK6 cell growth arrest and apoptosis through PARP-1/p53 regulatory pathway. *Environ. Toxicol.* 32, 2163–2171.
- Moll, U.M., Petrenko, O., 2003. The MDM2-p53 interaction. *Mol. Canc. Res.* 1, 1001–1008.
- Mandal, A., Bennett, L.L., 2016. Resveratrol enhances the efficacy of sorafenib mediated

- apoptosis in human breast cancer MCF7 cells through ROS, cell cycle inhibition, caspase 3 and PARP cleavage. *Biomed. Pharmacother.* 84, 1906–1914.
- Nachshon-Kedmi, M., Yannai, S., Haj, A., Fares, F.A., 2003. Indole-3-carbinol and 3,3'-diindolylmethane induce apoptosis in human prostate cancer cells. *Food Chem. Toxicol.* 41, 745–752.
- Ogawara, Y., Kishishita, S., Obata, T., Isazawa, Y., Suzuki, T., Tanaka, K., Masuyama, N., Gotoh, Y., 2002. Akt enhances Mdm2-mediated ubiquitination and degradation of p53. *J. Biol. Chem.* 277, 21843–21850.
- Pancholi, S., Lykkesfeldt, A.E., Hilmi, C., Banerjee, S., Leary, A., Drury, S., Johnston, S., Dowsett, M., Martin, L.A., 2008. ERBB2 influences the subcellular localization of the estrogen receptor in tamoxifen-resistant MCF-7 cells leading to the activation of AKT and RPS6KA2. *Endocr. Relat. Canc.* 15, 985–1002.
- Rane, M.J., Pan, Y., Singh, S., Powell, D.W., Wu, R., Cummins, T., Chen, Q., McLeish, K.R., Klein, J.B., 2003. Heat shock protein 27 controls apoptosis by regulating Akt activation. *J. Biol. Chem.* 278, 27828–27835.
- Rathore, S., Datta, G., Kaur, I., Malhotra, P., Mohmmmed, A., 2015. Disruption of cellular homeostasis induces organelle stress and triggers apoptosis like cell-death pathways in malaria parasite. *Cell Death Dis.* 6, e1803.
- Rogers, C., Fernandes-Alnemri, T., Mayes, L., Alnemri, D., Cingolani, G., Alnemri, E.S., 2017. Cleavage of DFNA5 by caspase-3 during apoptosis mediates progression to secondary necrotic/pyroptotic cell death. *Nat. Commun.* 8, 14128.
- Sarto, C., Binz, P.A., Mocarelli, P., 2000. Heat shock proteins in human cancer. *Electrophoresis* 21, 1218–1226.
- Shen, J., Wu, Y., Xu, J.Y., Zhang, J., Sinclair, S.H., Yanoff, M., Xu, G., Li, W., Xu, G.T., 2010. ERK- and Akt-dependent neuroprotection by erythropoietin (EPO) against glyoxal-AGEs via modulation of Bcl-xL, Bax, and BAD. *Invest. Ophthalmol. Vis. Sci.* 51, 35–46.
- Sherer, C., Tolaymat, I., Rowther, F., Warr, T., Snape, T.J., 1 April 2017. Preliminary SAR on indole-3-carbinol and related fragments reveals a novel anticancer lead compound against resistant glioblastoma cells. *Bioorg. Med. Chem. Lett.* 27 (7), 1561–1565.
- Souli, E., Machluf, M., Morgenstern, A., Sabo, E., Yannai, S., 2008. Indole-3-carbinol (I3C) exhibits inhibitory and preventive effects on prostate tumors in mice. *Food Chem. Toxicol.* 46, 863–870.
- Srinivas, P.R., Verma, M., Zhao, Y., Srivastava, S., 2002. Proteomics for cancer biomarker discovery. *Clin. Chem.* 48, 1160–1169.
- Surget, S., Khoury, M.P., Bourdon, J.C., 2013. Uncovering the role of p53 splice variants in human malignancy: a clinical perspective. *Oncotargets Ther.* 7, 57–68.
- Tian, X., Zhao, L., Song, X., Yan, Y., Liu, N., Li, T., Yan, B., Liu, B., 2016. HSP27 inhibits homocysteine-induced endothelial apoptosis by modulation of ROS production and mitochondrial caspase-dependent apoptotic pathway. *BioMed Res. Int.* 2016 4847874.
- Vizotto-Duarte, C., Custodio, L., Gangadhar, K.N., Lago, J.H., Dias, C., Matos, A.M., Neng, N., Nogueira, J.M., Barreira, L., Albericio, F., Rauter, A.P., Varela, J., 2016. Isololiolide, a carotenoid metabolite isolated from the brown alga *Cystoseira tamiscifolia*, is cytotoxic and able to induce apoptosis in hepatocarcinoma cells through caspase-3 activation, decreased Bcl-2 levels, increased p53 expression and PARP cleavage. *Phytomedicine* 23, 550–557.
- Wang, X., Chen, M., Zhou, J., Zhang, X., 2014. HSP27, 70 and 90, anti-apoptotic proteins, in clinical cancer therapy (Review). *Int. J. Oncol.* 45, 18–30.
- Wurstle, M.L., Laussmann, M.A., Rehm, M., 2012. The central role of initiator caspase-9 in apoptosis signal transduction and the regulation of its activation and activity on the apoptosome. *Exp. Cell Res.* 318, 1213–1220.